Quantum Cascade Phenomenon in $Bi_2Sr_2CaCu_2O_{8+\delta}$ Single Crystals

V. M. Krasnov

Department of Physics, Stockholm University, AlbaNova University Center, SE-10691 Stockholm, Sweden
(Received 21 August 2006; published 19 December 2006)

We study interlayer transport in $Bi_2Sr_2CaCu_2O_{8+\delta}$ cuprates, which represent stacks of atomic scale intrinsic Josephson junctions. A series of resonant dips in conductance is observed at condition when bremsstrahlung and recombination bands in nonequilibrium spectrum of Josephson junctions overlap. The phenomenon is explained in terms of self-detection of a new type of collective strongly nonequilibrium state in natural atomic superlattices, bearing certain resemblance with operation of a quantum cascade laser. Conclusions are supported by *in situ* generation-detection experiments and by numerical simulations.

Superlattices have become an essential part of modern electronics and optics [1,2]. One of superlattice-based devices is a quantum cascade laser (QCL) [1], in which a superlattice forms a stack of tunnel junctions. Sequential tunneling in the stack creates nonequilibrium electron distribution (population inversion) and facilitates cascade amplification of radiation. Both processes are central to laser action. While fabrication of homogeneous superlattices is a formidable task [3], atomically perfect superlattices are naturally formed in certain layered compounds [4–7]. Properties of those compounds can be varied by intercalation [4,8] and doping [9], allowing flexibility, similar to band engineering in semiconductor superlattices [1,3]. Figure 1(a) shows the crystallographic structure of $Bi_2Sr_2CaCu_2O_{8+\delta}$ (Bi-2212) high T_c superconductor (HTSC), which represents a natural stack of atomic scale "intrinsic" Josephson junctions (IJJ's) [5,8,10–13].

Here we study interlayer transport in small Bi-2212 mesa structures. A new phenomenon, seen as a series of resonant dips in interlayer conductance at multiples of the sum-gap voltage, is observed. It is concluded that the phenomenon represents a new type of collective strongly nonequilibrium state in stacked IJJ's, bearing certain resemblance with operation of the QCL.

To study interlayer transport, small mesa structures containing few atomic layers were microfabricated on top of Bi-2212 single crystals. Figure 1(b) represents a sketch of a triple-mesa structure used for *in situ* generation-detection experiments. It consists of generator and detector mesas (*B* and *C*) on top of a common pedestal (*D*) and several single mesas *A*, *E* required for independent biasing of *B*, *C*. Mesas *B* and *C* were obtained by cutting the initial mesa *D* with focused ion beam. This allows nanoscale separation between mesas *B* and *C*, needed for *in situ* detection [14]. Details of sample fabrication are described elsewhere [13].

Figure 1(c) shows a current-voltage characteristic (IVC) at $T = 4.2$ K for a single mesa on a slightly overdoped crystal with $T_c = 92.5$ K. Multibranch structure is due to one-by-one switching of IJJ's in the resistive state. Figures 1(d) and 1(e) show IVC's of a triple mesa on a near optimally doped crystal, $T_c = 93.6$ K, measured in

three- ($I^+ = V^+ = B$, $I^- = A$, $V^- = E$) and four-probe ($I^+ = B$, $V^+ = C$, $I^- = A$, $V^- = E$) configurations, respectively. The pedestal mesa *D* had an area $4 \times 5 \ \mu m^2$; mesas *B* and *C* had areas $4 \times 2.25 \ \mu m^2$, and were separated by 0.5 μm. In the three probe configuration the IVC is a sum of IVC's of mesas *B* and *D*, as seen from appearance of two families of branches with a difference in critical currents determined by the ratio of areas of mesas *B* and $D \simeq 0.45$.

Figure 2(a) shows tunneling conductance $\sigma = dI/dV(V)$ at $T < T_c$. A smooth normal state characteristic at $T = 100$ K was subtracted to improve resolution [9]. IVC's of single mesas have the shape typical for superconductor-insulator-superconductor (SIS) tunnel junctions with a sharp peak in conductance at the sum-gap voltage $V_g = 2\Delta/e$ per junction, where Δ is the superconducting energy gap [8,9,12]. Improved resolution allows for the first time observation of a fine structure at high bias: arrows in Fig. 2(a) indicate appearance of dips in dI/dV at $V > V_g$. Those features can be clearly seen in the second derivative plot $d^2I/dV^2(V)$, shown in Fig. 2(b) for a slightly underdoped mesa, $T_c = 88$ K. Here up to three kinks above V_g can be distinguished.

Figures 2(c) and 2(d) show T dependencies of peak and dip voltages per IJJ. In Fig. 2(d) data for another mesa on the same crystal are also included to demonstrate reproducibility of the features. Lines in Fig. 2(c) indicate that the two consecutive dips in dI/dV occur at $V = 2V_g$ and $3V_g$, respectively. In Fig. 2(d) up to three dips are observed in a wide T range. Here dips occur at V slightly smaller than multiples of V_g: by 10% for the line $\sim 4\Delta/e$, and by 15% for lines $\sim 6\Delta/e$ and $\sim 8\Delta/e$. Such deviations can be attributed to self-heating at large bias [14].

So far peculiarities at multiples of V_g were not reported neither for single nor stacked Josephson junctions. On the other hand, peculiarities in nonequilibrium phonon distribution at the corresponding voltages have been observed in phonon generation-detection experiments [15–19]. In that case a second SIS junction (the detector) was connected to the biased junction (the generator). The quasiparticle (QP)
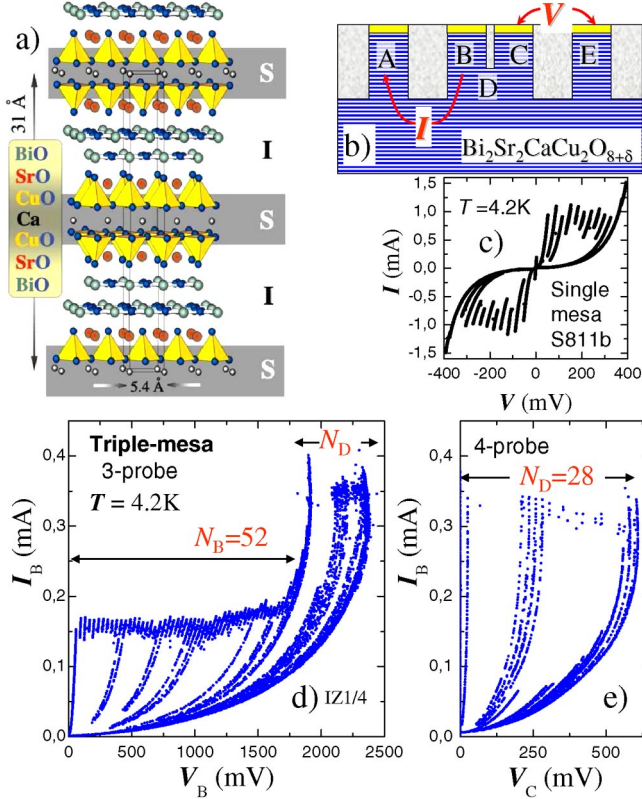
FIG. 1 (color online). (a) The crystallographic structure of Bi-2212 (after A. Yurgens). Mobile charge carriers are confined to $(CuO_2\text{-}Ca\text{-}Cu0_2)$ planes. Tunneling through (SrO-2BiO-SrO) layers leads to appearance of intrinsic junctions with the stacking periodicity 15.5 Å. (b) Sketch of a triple-mesa structure. Contact configuration used in four-probe measurements is shown. (c) IVC's of a single mesa (c) and a triple mesa in (d) three- and (e) four-probe configurations. Two families of branches, originating from IJJ's in mesas B and D, with ~0.45 difference in the critical current, are seen in (d). The four-probe IVC in (e) contains only branches from the mesa D.
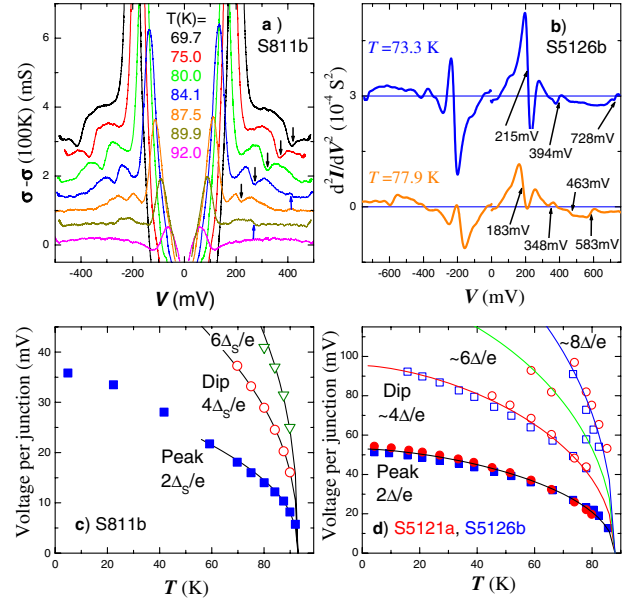

FIG. 2 (color online). (a) Tunneling conductance $dI/dV(V)$ for the same single mesa as in Fig. 1(c). The peak at $V_g = 2\Delta/e$ per IJJ is the dominant feature of the spectra. Downwards and upwards arrows indicate main and secondary dips in dI/dV, respectively. (b) The second derivative $d^2I/dV^2(V)$ curves at two $T < T_c$ for an underdoped mesa. Curves at different T in (a), (b) were shifted for clarity. Panels (c), (d) show T dependencies of the peak (solid symbols) and the dips (open symbols) in dI/dV for (c) the overdoped mesa and (d) two mesas on the same underdoped crystal. Lines represent the fit to the peak voltage (the lower line) and multiple integers of that. Coincidence of the lines with open symbols indicate that dips occur at voltages, $V \simeq 2(n + 1)\Delta/e$ ($n = 1, 2, 3$), per junction.

conductance of the detector increased stepwise at $V = nV_g$ in the generator, due to excess flow of nonequilibrium phonons with energy $\Omega > 2\Delta$, sufficient for Cooper pair breaking in the detector. However, no peculiarities in the generator itself were reported. Also conductance in Fig. 2(a) exhibits resonant dips rather than steps. This difference is related to the specific sample geometry: in classical generation-detection experiments the generator was biased independently from the detector and always remained in a quasiequilibrium state. To the contrary, in our case the signal is due to collective self-detection in simultaneously biased stacked junctions, which all may be in a strongly nonequilibrium state.

To understand nonequilibrium processes in stacked Josephson junctions, let us consider the diagram in Fig. 3(a). Tunneling leads to nonequilibrium population of QP's with maximum at $E = eV - \Delta$. The decay of QP's typically follows a two-step process [18]. First QP's relax to the bottom of the empty band, emitting a bremsstrahlung

(braking) radiation [16]. At the second stage, two QP's from the bottom of the band recombine into the Cooper pair, emitting recombination radiation. The process is repeated in the next junction leading to cascade amplification of radiation in the stack, as illustrated by wavy arrows in Fig. 3(a).

Emission of a boson with frequency Ω due to relaxation of a QP with energy E occurs at the rate [20]

$$\frac{\partial g}{\partial t} \propto \rho(E)\rho(E - \Omega)f(E)[1 - f(E - \Omega)][1 + g(\Omega)], \quad (1)$$

where ρ is the QP density of states, and g and f are distribution functions for bosons and QP's, correspondingly. Factors 1 and $g(\Omega)$ in the last term represent probabilities of spontaneous and stimulated emissions, respectively.

Figure 3(b) shows calculated spectrum of nonequilibrium phonons for a single junction at $V = 3.5\Delta/e$; see Ref. [21]. Two discrete phonon bands with abrupt cutoffs at $\Omega_B \leq eV - 2\Delta$ for braking and $\Omega_R \geq 2\Delta$ for recombination bands are seen. Spectra are peaked at the band edges, indicating the two most probable QP decaying events. At $V \geq 4\Delta/e$ the two bands overlap. Now high frequency braking phonons with $\Omega_B \geq 2\Delta$ can split Cooper pairs and generate secondary QP's. Relaxation of such QP's
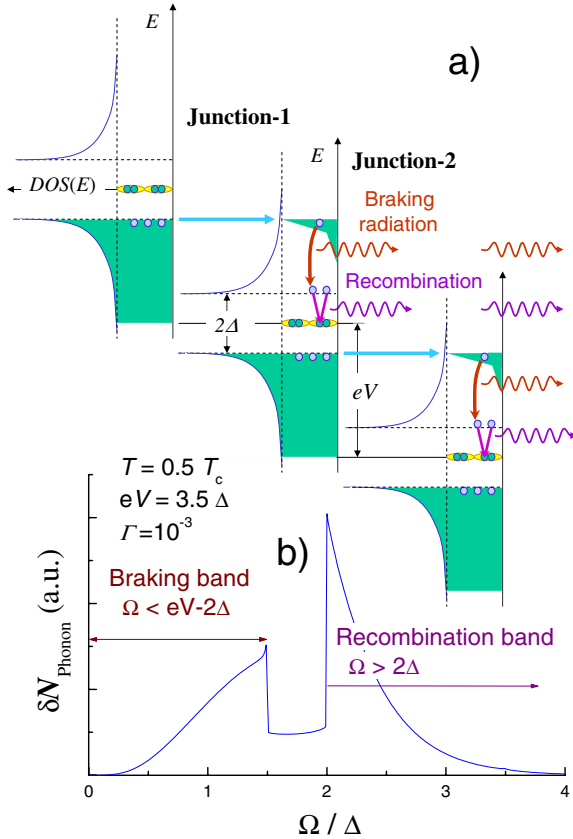
FIG. 3 (color online). (a) A schematic energy diagram of two stacked SIS junctions biased at voltage V per junction. For $V \geq 2\Delta/e$ tunneling results in nonequilibrium QP population in the empty band. Arrows indicate the most probable relaxation scenario of QP's. The process is repeated in the second junction, resulting in cascade amplification of radiation, as indicated by wavy arrows. (b) Calculated number of nonequilibrium phonons for a single SIS junction, biased at $V = 3.5\Delta/e$. Two phononic bands are clearly seen. The two bands overlap at $V = 4\Delta/e$, corresponding to the first dip in $dI/dV(V)$ from Fig. 2(a).

leads to appearance of secondary braking bands with

$$\Omega_B \leq eV - 2(1 + m)\Delta, \qquad (m = 0, 1, 2, \ldots). \qquad (2)$$

Here m is the number of secondary relaxation stages [18].

From Figs. 2(c) and 2(d) and Eq. (2) it follows that the dips occur upon collision of the recombination band with one of the braking bands. According to Eq. (1), this may accelerate emission at the overlap frequency, $\Omega = 2\Delta$, due to stimulated emission. But stimulated emission is significant only if strongly nonequilibrium population $g(\Omega)$ was initially present in the bands. Normally, this does not occur in single Josephson junctions. However, in stacked junctions strong disequilibrium can be achieved due to cascade amplification of radiation. The amplification is efficient only if junctions in the stack are identical. Indeed, the dips were pronounced only in mesas with identical IJJ's. High uniformity of our mesas can be seen from the periodicity of multibranch IVC's in Fig. 1. It can also be seen

from the sharpness of the peak in Fig. 2(a), which indicates [22] that all IJJ's reach V_g at the same I. In experiment, a correlation between the height of the peak at V_g and the depth of the dip at $2V_g$ was observed.

To independently study nonequilibrium radiation, generation-detection experiments were carried out using the triple-mesa structure, shown in Fig. 1. Figure 4(a) shows current density versus voltage-per-junction characteristics of the triple mesa D at $T = 75.2$ K and for a single mesa A on the same crystal at two nearby T. Areas of mesas A and B [through which the current was applied in the triple-mesa structure, see Fig. 1(b)] were the same, $A_A = A_B = 4 \times 2.25~\mu\text{m}^2 \simeq 0.45 A_D$. For identical IJJ's the $J(V/N)$ characteristics should be independent of the mesa geometry. Indeed, it is seen that at low bias the characteristics of mesa D coincides with that of mesa A at $T = 74.9$ K; for high bias it is similar in shape to that of mesa A at slightly higher $T = 79.3$ K, indicating a minor self-heating from the mesa B [14]. Both observations confirm that IJJ's in mesas A and D are similar. However, while the IVC's of the single mesa A exhibit the conventional kink at V_g, the IVC of the triple mesa suddenly drops to a smaller V. The arrow in Fig. 4(a) indicates that the drop is coaligned with the kink in $J(V/N)$ of mesa A. Therefore, it occurs when IJJ's in mesa D reach the sum-gap bias.

Figure 4(b) shows four-probe $dI/dV(I)$ curves for the same triple mesa at $T = 65$ K. Here correlation between the voltage drop ($dI/dV \simeq 0$ at 1.1 mA $< I <$ 1.2 mA) and the peak at the sum-gap bias, I_p, in mesa D can be seen explicitly. Noticeably, an additional peak, never observed in single mesa characteristics, occurs at $I = 0.45 I_p$, corresponding to the sum-gap bias in mesa B.

Thus, a specific response in the detector mesa C occurs when IJJ's in both generator mesas B and D reach the sum-gap bias. It should be emphasized that the response is not due to QP injection because the mesa C is unbiased and the QP current in mesas B and D changes gradually through the singularities. Therefore, the singularities indicate appearance of strong recombination radiation in IJJ's of mesas B and D when they reach V_g. This recombination radiation, $\Omega_R \geq 2\Delta$, results in partial depairing and increase of QP population in mesa D, which is sensed by the detector C. Since only the generator D is in direct contact with the detector C, the response from D is stronger (discontinuity in the IVC) than from B (peak in the derivative). The response can be attributed to appearance of in-plane resistance between mesas B and C [23], and to imbalance in QP population between mesas D and C [24], leading to appearance of negative voltage at mesa C similar in origin to the built-in potential in n-p junctions. Both types of responses enhance with increasing depairing in mesa D.

A closer examination of triple-mesa IVC's reveals that the voltage drop, see Fig. 4(c), consists of a set of tiny subbranches. Their number is approximately equal to the number of IJJ's in the mesa D. This indicates that nonequi-
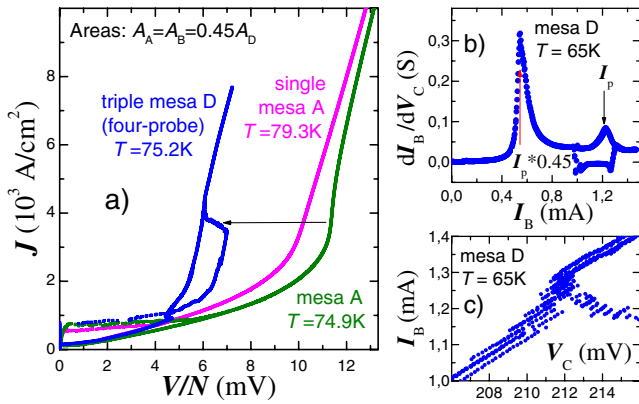
FIG. 4 (color online). (a) Current density vs voltage-per-junction characteristics for the pedestal mesa D in the triple-mesa structure (blue curve) and for a single mesa A on the same crystal. A sudden drop in the IVC of mesa D is seen. Comparison with mesa A demonstrates that the drop occurs when IJJ's in mesa D reach the sum-gap bias, as indicated by the arrow. (b) Four-probe $dI_B/dV_C(I_B)$ characteristics for the triple mesa at $T = 65$ K [subscripts indicate contact configurations according to Fig. 1(b)]. Two peaks are observed, unlike for single mesas. The peak marked I_p corresponds to the sum-gap bias in mesa D and is associated with the voltage drop ($dI/dV \simeq 0$ at $I \sim 1.1$–1.2 mA). The peak at $I = 0.45I_p$ corresponds to the sum-gap bias of the mesa B. Those peculiarities measured at the unbiased detector mesa C indicate appearance of strong recombination radiation when either mesas B or D reach the sum-gap bias. (c) Enlarged part of the drop in the triple-mesa IVC at $T = 65$ K, demonstrating presence of tiny sub-branches, indicating that the nonequilibrium state in the stack is amplified in a cascade manner when IJJ's in mesa D sequentially reach the sum-gap bias.

librium radiation is amplified in a cascade manner each time an additional IJJ in mesa D reaches V_g.

To summarize, we observed a new phenomenon in interlayer characteristics of Bi-2212 single crystals. It is seen as a set of resonant dips in conductance at multiples of the sum-gap voltage $2(n + 1)\Delta/e$, $n = 1, 2, 3$, at which bremsstrahlung and recombination bands in nonequilibrium spectrum of Josephson junctions overlap. *In situ* generation-detection experiments provided evidence for strong recombination radiation and for cascade amplification of radiation in stacked IJJ's. This brings us to the conclusion that the phenomenon represents a new type of collective nonequilibrium state in the natural atomic superlattice, which bears certain resemblance with operation of the QCL. As in the QCL, nonequilibrium QP population is created by interlayer tunneling and stimulated emission is achieved by cascade amplification of radiation in the stack. On the other hand, emission in Bi-2212 is conceptually different from the QCL: (i) emitted are not photons but other bosons (e.g., phonons or spin waves), coupled to superconducting QP's. (ii) The band gap is not due to level quantization in a quantum well, but is the superconducting energy gap. Whence, the phenomenon disappears at $T >$

T_c. (iii) Stimulated emission occurs when bosonic, rather than electronic, bands overlap. Since the overlap frequency, $\Omega = 2\Delta$, is sufficient for pair braking, it leads to resonant suppression of superconductivity, resulting in the drop of conductance to approximately the normal state value, as seen from Fig. 2(a).

Our observation has several interesting implications: (i) it can be important for understanding HTSC. Bosonic excitations mediating superconductivity are emitted upon recombination of QP's (e.g., phonons are emitted in conventional superconductors). Therefore, identification of nonequilibrium radiation emitted by IJJ's may disclose the coupling mechanism of HTSC. (ii) So far superlattice devices relied on complicated fabrication of artificial multilayers. Our data show that similar phenomena may occur in natural atomic superlattices. This may open a possibility for building electronics at the ultimate atomic scale.

[1] J. Faist *et al.*, Science **264**, 553 (1994).
[2] S. A. Wolf *et al.*, Science **294**, 1488 (2001).
[3] P. Offermans *et al.*, Appl. Phys. Lett. **83**, 4131 (2003).
[4] A. H. Thompson, F. R. Gamble, and R. F. Koehler, Phys. Rev. B **5**, 2811 (1972); R. C. Morris and R. V. Coleman, Phys. Rev. B **7**, 991 (1973).
[5] R. Kleiner and P. Müller, Phys. Rev. B **49**, 1327 (1994).
[6] T. Nachtrab *et al.*, Phys. Rev. B **65**, 012410 (2001).
[7] Yu. I. Latyshev *et al.*, J. Phys. A **36**, 9323 (2003).
[8] V. M. Krasnov *et al.*, Phys. Rev. Lett. **86**, 2657 (2001).
[9] V. M. Krasnov, Phys. Rev. B **65**, 140504 (2002).
[10] V. M. Krasnov *et al.*, Phys. Rev. B **59**, 8463 (1999).
[11] H. B. Wang *et al.*, Phys. Rev. Lett. **87**, 107002 (2001).
[12] V. M. Krasnov *et al.*, Phys. Rev. Lett. **84**, 5860 (2000).
[13] V. M. Krasnov, T. Bauch, and P. Delsing, Phys. Rev. B **72**, 012512 (2005).
[14] V. M. Krasnov, M. Sandberg, and I. Zogaj, Phys. Rev. Lett. **94**, 077003 (2005).
[15] W. Eisenmenger and A. H. Dayem, Phys. Rev. Lett. **18**, 125 (1967).
[16] H. Kinder, Phys. Rev. Lett. **28**, 1564 (1972); P. Berberich, R. Buemann, and H. Kinder, Phys. Rev. Lett. **49**, 1500 (1982).
[17] A. H. Dayem and J. J. Wiegand, Phys. Rev. B **5**, 4390 (1972).
[18] I. E. Singer and W. E. Bron, Phys. Rev. B **14**, 2832 (1976).
[19] R. C. Dynes and V. Narayanamurti, Phys. Rev. B **6**, 143 (1972).
[20] J. J. Chang and D. J. Scalapino, Phys. Rev. B **15**, 2651 (1977).
[21] See EPAPS Document No. E-PRLTAO-97-032651 for details of calculations for the spectrum in Fig. 3(b). For more information on EPAPS, see http://www.aip.org/pubservs/epaps.html.
[22] V. M. Krasnov, Physica (Amsterdam) **372–376C**, 103 (2002).
[23] L. X. You *et al.*, Supercond. Sci. Technol. **17**, 1160 (2004); Phys. Rev. B **71**, 224501 (2005).
[24] S. Rother *et al.*, Phys. Rev. B **67**, 024510 (2003).